Rendiconti Lincei. Scienze Fisiche e Naturali (2019) 30:399–415
https://doi.org/10.1007/s12210-019-00803-x

Petrographic and chemical characterization of Middle Bronze Age pottery from Sicily: towards a definition of an Etnean production

D. Tanasi[1] · G. Caso[2] · R. H. Tykot[2] · D. Amoroso[3]

Received: 16 February 2019 / Accepted: 30 March 2019 / Published online: 7 May 2019

Abstract
The Middle Bronze Age in Sicily (fifteenth–thirteenth century BC) represents a crucial moment in the evolution of Prehistoric pottery production. However, the scarcity of specific petrographic and chemical studies has represented until now a serious interpretative handicap for archeologists. The recent study of two important Middle Bronze Age pottery complexes from the Etnean area (Grotte di Marineo di Licodia Eubea and Monte San Paolillo di Catania) has offered the possibility to add new significant data to characterize the manufacturing practices behind such production. A new assemblage of Thapsos pottery from the Middle Bronze Age site of St. Ippolito hill at Caltagirone can shed new light on the features of such Etnean production. This paper highlights the potential of the application of an array of techniques such as petrographic analysis of thin sections and chemical analyses via X-ray fluorescence spectrometry and electron microprobe analysis to better investigate production technology of Middle Bronze Age Sicilian pottery.

Keywords Sicily · Middle Bronze Age · Pottery technology · Petrography · pXRF · EPMA

1 Introduction

The Sicilian Middle Bronze Age (MBA), identified with the Thapsos culture (fifteenth–thirteenth century BC), represents the most important phase of the Bronze Age with respect to the emergence of a common technological *koine* for pottery production, characterized by new ways of clay procurement strategies, pottery-making practices, and firing technology (Cuomo di Caprio 2007; Bietti Sestieri 2015; Borgna and Levi 2015). Such a technological *koine* will be fully established only later in the course of the subsequent Late Bronze Age (LBA) culture of North Pantalica (thirteenth–eleventh century BC) (Tanasi 2008). The circulation of Mycenaean pottery and the contact with foreign and more skilled potters triggered an intense period of experimentalism by local artisans, which resulted in various districts' production of Siracusan and Etnean Thapsos (Alberti 2013, 2017; Bietti Sestieri 2015; Jones et al. 2014; Russell 2017; Tusa 2000).

After a series of traditional studies which tackled the typological classification of the Thapsos pottery (Alberti 2004, 2008; Tanasi 2008, 2010a, 2015; Veca 2014a, b, 2015), in the last few years new research focused on the technical aspects of the ceramic production using as a case study the evidence from the territory of Catania, in particular from the sites of Monte San Paolillo di Catania and Grotte di Marieneo di Licodia Eubea.

At the core of these technological changes, two main shifts within the production strategies adopted by local communities can be placed. On the one hand, during the second half of the MBA, there is an increasing interest towards high-calcium-oxide-based clays, which will become more common than alluvial clays in use during the earliest part of the MBA (Barone et al. 2011a, b, 2012; Raneri et al. 2015a, b; Rodrıguez et al. 2015, Tanasi et al. 2013; Veca 2014a, b,

✉ G. Caso
gianpiero@usf.edu

D. Tanasi
dtanasi@usf.edu

R. H. Tykot
rtykot@usf.edu

D. Amoroso
d-amoroso@virgilio.it

[1] Department of History, University of South Florida, Tampa, Florida, USA

[2] Department of Anthropology, University of South Florida, Tampa, Florida, USA

[3] Musei Civici Luigi Sturzo, Caltagirone, Italy

2015). On the other hand, such a change in the clay procurement is also accompanied by a change in firing techniques, which started to rely on kilns with underneath chambers instead of those with a side chamber, thus reaching very high temperatures (> 900 °C) during the latest phases of the MBA (Borgna and Levi 2015; Cultrone et al. 2001; Jones et al. 2014; Raneri et al. 2015b).

The opportunity to expand the range of data at our disposal and to attempt a more in-depth analysis of the Thapsos pottery production in the territory of Catania comes from the reassessment of a large assemblage of ceramics collected during excavations undertaken by the Musei Civici "Luigi Sturzo" of Caltagirone in the late 1990s on the hill of St. Ippolito at Caltagirone. The combination of both chemical and petrographic analyses of the mineral composition of ceramics from the hill of Sant'Ippolito has the potential of exploring and assessing some aspects of local ceramic production during the Middle Bronze Age of eastern Sicily.

After more than 10 years since its recovery, the ceramic assemblage from Caltagirone has finally become the focus of an interdisciplinary study aimed at detecting, examining, and defining the occupation of the hill, spanning throughout the MBA and the early LBA. The goal is to tackle the discussion concerning the main technological features of Thapsos ceramics in the Caltagirone area, to understand the practices that were commonly accepted by such a large community within the broader geographical context of southeastern Sicily, and ultimately to define the local ceramic production and distribution.

Although this portion of the island is very well known to archeologists for the widespread presence of several social groups sharing similar cultural and technological practices during that period, almost no information has been published yet for the westernmost part of the Hyblean Platform at the time of the Thapsos culture. Against this picture, the case study of Sant'Ippolito may provide additional new data.

2 The case study of St. Ippolito Hill

The Hill of Sant'Ippolito at Caltagirone is not new to the archeological literature, being strictly connected with the first discovery of an important eponymous Copper Age pottery style (Crispino and Ippolito 2014). During excavations carried out in the 1990s, the important evidence of a Middle Bronze Age (1550–1250 BC) settlement emerged (Amoroso 1987). The site also showed a later phase of use, represented by a low stone precinct surrounding a floor lever with a hearth by which a fragment of a terracotta stove and a cooking jar were found, dated to the Early Iron Age (1050–950 BC) (Tanasi et al. 2017). In the frame of an overall reappraisal of the archeological evidence from this excavation, still unpublished at this point, a research project with a strong archeometric component has recently been carried out (Caso et al. 2017), which also led to the reappraisal of the stratigraphic deposit and the related ceramic materials.

Without entering into the details of the results of the excavation, which will be the subject of another publication currently under preparation, it is possible to see in the aerial view of St. Ippolito (Fig. 1) how the hill comprises an upper hill and a lower hill, and how its original profile and shape were drastically transformed by the activities connected to a gypsum quarry. The hypothetical location of the Copper Age site identified by Paolo Orsi when he first investigated the site (Crispino and Ippolito 2014) should be in the valley between the San Giorgio River and the St. Ippolito Hill itself. The excavation carried out in the 1990s focused on the lower terrace, where two large trenches were opened (Saggio A and Saggio B). While Saggio A provided just data about an occupation dated to the Greek Archaic period, Saggio B offered evidence of a consistent occupation mostly during the Middle Bronze Age and poorer traces of use in the Late Bronze Age and Early Iron Age, with remnants of huts. The floor level of similar huts was and still is visible both in the upper and the lower terraces (purple dots in Fig. 1). The Saggio B comprises 17 quadrants of irregular sizes ranging from 2.50 to 1.50 m, added progressively one after the other. As emphasized in Fig. 2, better preserved structures associated with diagnostic materials dated to the Early Iron Age were identified in quadrants 10/8/5/17 (Tanasi et al. 2017) and remnants of two superimposed Bronze Age structures were found in quadrant 4, which produced the most complete stratigraphic sequence (Fig. 3). The vast majority of the ceramics recovered in Saggio B were of Thapsos type and represent the three main sub-phases of this production: I, II, III (Alberti 2017) (Fig. 4).

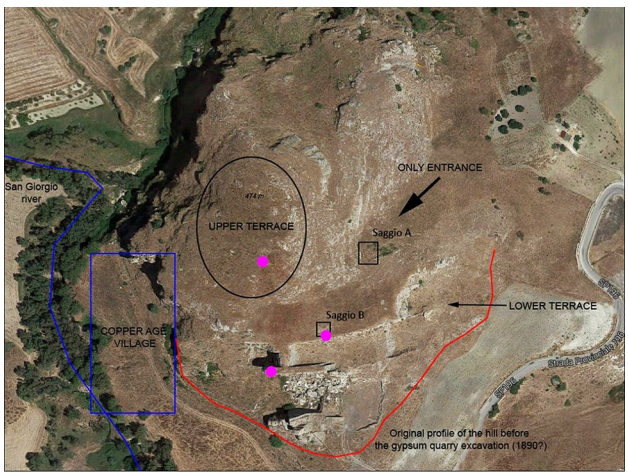

Fig. 1 Aerial view of St. Ippolito Hill with indication of the two main excavation areas

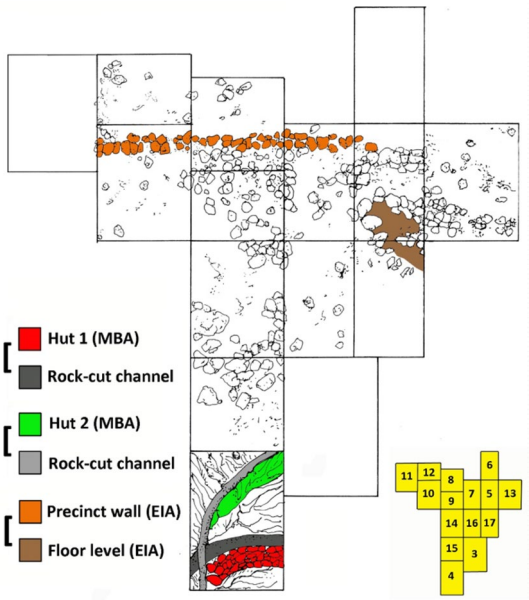

Fig. 2 Schematic plan of the main chronological phases of the structured uncovered in Saggio B (Caso et al. 2017)

3 Materials

The traditional assessment by archeologists of the Thapsos pottery from Sant'Ippolito via direct examination led to the identification of six main fabrics on the basis of parameters such as texture, manufacture, and function (Table 1): very fine hard fabric with smoothed and burnished surface (fabric I); fine hard fabric with smoothed and painted surface (fabric II); fine hard fabric with smoothed and undecorated surface (fabric III); coarse soft fabric with a rough and rarely slipped surface (fabric IV); medium soft and undecorated fabric (fabric V); and coarse medium fabric with unsmoothed (fabric VI) which occurs only on large storage jars.

To test the validity of the initial fabric classification and to better understand the relationship between fabrics and typologies, a group of 23 Thapsos pottery samples representing the most common shape types and fabrics was sampled for archeometric analyses. To this group, four samples of cooking plates and adobe from the same stratigraphic context where the other samples came from were added together with two samples taken from later North Pantalica vessels to define possible technological changes at the transition between the two periods, for a total of 29 samples (Table 2; Fig. 5).

4 Methods

Samples were subject to an array of optical and chemical comparative analyses to enhance the quality of the data gathered to either confirm or reject the interpretation given by archeologists concerning pottery fabrics (Table 3).

4.1 Petrographic analysis of thin sections

Among the entire group of samples, 17 most representative specimens were selected for the petrographic study (USF29350, 29351, 29354, 29355, 29357, 29358, 29359, 29360, 29361, 29362, 29363, 29365, 29368, 29369, 29370, 29376, 29377), to either confirm or reject the interpretation provided by the direct examination of the fabrics. Thin section production was carried out in the Department of Geosciences at the University of South Florida. Thin sections were described using an Olympus B120C polarizing microscope, following the standards proposed by Whitbread (1989), Quinn (2013), and Santacreu (2014).

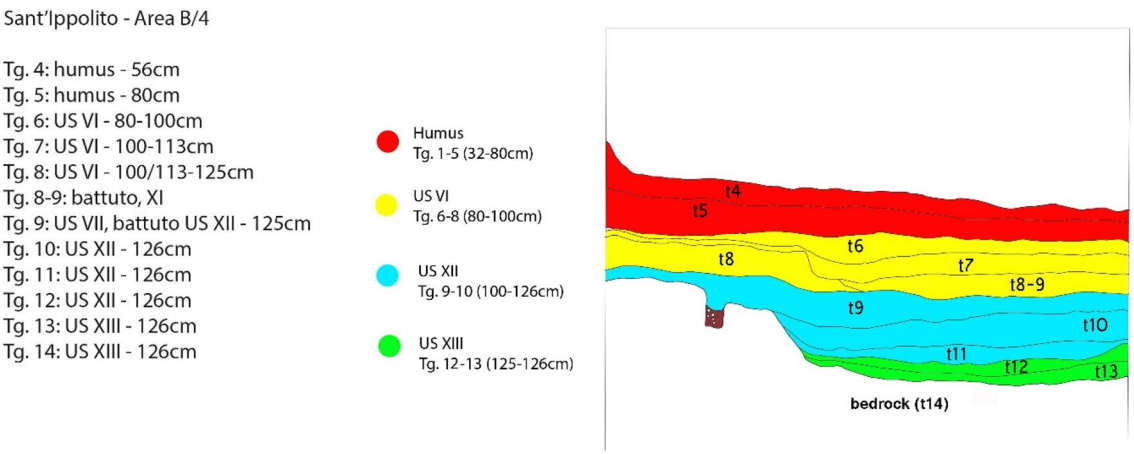

Fig. 3 Saggio B, quadrant 4, section view North–South (elaborated by authors)

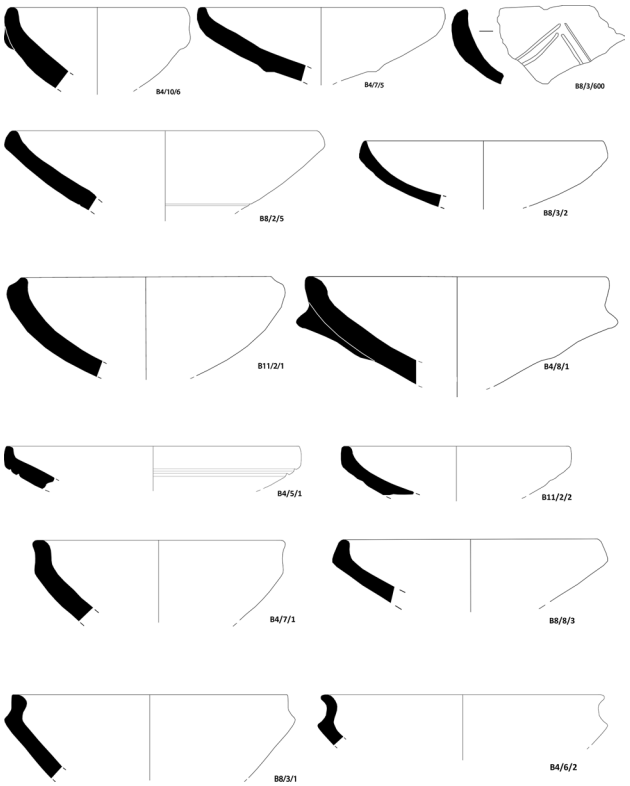

Fig. 4 Saggio B, assemblage of Thapsos pottery of sub-phases I, II, and III (drawings C. Veca and G. Caso), scale 1:2

By doing so, a new classification for the samples can be proposed, according to specific features of the ceramics including the structure of the clay paste, grain size and distribution, and overall texture. The resulting groups are, therefore, established according to the parameters that have been used in the literature to explain technological features related to manufacture and firing techniques of pottery production throughout the broader geographical context of the eastern side of Sicily (Barone et al. 2011a, b, 2012; Raneri et al. 2015a, b; Rodriguez et al. 2015; Tanasi et al. 2013).

4.2 Chemical analysis with a portable X-ray fluorescence spectrometer

The chemical analysis of the selected samples was carried out at the Laboratory for Archaeological Science & Technology (LAST) in the Department of Anthropology at the University of South Florida using a Bruker Tracer III-SD X-ray fluorescence spectrometer.

The analysis was performed with settings of 40 kV and 10 μA, using a 12-μm Al, 1-μm Ti, and 6-μm Cu filter to minimize background and enhance measurements of peak areas (Emmitt et al. 2018; Forster et al. 2011; Newlander et al. 2015; Stovel et al. 2016), and according to the standards proposed by Hunt and Speakman (2015) and Tykot (2016).

Table 1 Main fabrics of Thapsos pottery found at St. Ippolito Hill, identified via direct examination

Fabric I	Fabric II	Fabric III
Very fine hard fabric, smoothed, slipped, and burnished outer surface; body color 10YR 6/3 light yellowish red, slip color from 10YR 8/1 white to 10YR 6/6 brownish yellow Tableware: cups	Fine hard fabric, smoothed surface, dark brown paint applied directly over the body, more rarely over a yellowish-gray slip; body color 10YR 5/1 gray, paint color 7.5YR 4/2 brown, slip color 10YR 6/6 brownish yellow Tableware: cups, dipper cups	Fine hard fabric, smoothed undecorated and slipped surface, overfired; body color 10YR 6/3 and 10YR 7/6 yellow Tableware: cups
Fabric IV	**Fabric V**	**Fabric VI**
Coarse soft fabric, rough surface, rarely slipped; body color 5YR 6/8 reddish yellow, slip color 10YR 7/4 very pale brown Coarse ware: jars, trays	Medium soft fabric, rough non-slipped and undecorated surface; body color 5YR 7/6 reddish yellow Cooking ware: cooking pans	Coarse medium fabric, unsmoothed surface; body color 10YR 5/1 gray, slip color 10YR 6/6 brownish yellow Large storage jars

Table 2 List of samples for this study, including sample IDs, type, and class

Materials	Inv. No.	Sample ID	Fabric	Shape
	B4/5/3	USF29349	Fabric I	Foot of a cup (North Pantalica)
	B9/2/1	USF29350	Fabric I	Tubular Foot
-	B11/4/1	USF29351	Fabric II	Handle
	SN90/1	USF29352	Fabric II	Cup
	SN90/2	USF29353	Fabric II	Upper Foot
	B4/7/6	USF29354	Fabric III	Cup
	B4/8/2	USF29355	Fabric III	Cup
	B4/8/5	USF29357	Fabric III	Cup
	B4/9/2	USF29358	Fabric III	Cup
	B4/14/4	USF29359	Fabric III	Tubular Foot
	B11/2/2	USF29360	Fabric III	Cup
	B4/2/2	USF29361	Fabric IV	Situla
	B8/3/4	USF29362	Fabric IV	Jar
	B9/3/1	USF29363	Fabric IV	Tray

Table 2 (continued)

	B13/2/3	USF29364	Fabric IV	Jar (North Pantalica)
	B14/3/2	USF29365	Fabric IV	Jar
	B17/2-3/1	USF29366	Fabric IV	Tray
	B4/3/1	USF29367	Fabric V	Cooking Pan
	SN1	USF29368	Fabric V	Cooking Pan
	SN2	USF29369	Fabric V	Cooking Pan
	SN3	USF29370	Fabric V	Cooking Pan
	SN4	USF29371	Fabric V	Cooking Pan
	B4/7	USF29372	Fabric VI	Storage Jar
	B13/14/7	USF29373	Fabric VI	Storage Jar
	B4/8	USF29374	Fabric VI	Storage Jar
-	B14/6/SIP1	USF29375		Adobe
	B4/8/SIP2	USF29376		Cooking Plate
	B4/11/SIP3	USF29377		Cooking Plate
	B5/4/SIP4	USF29378		Cooking Plate

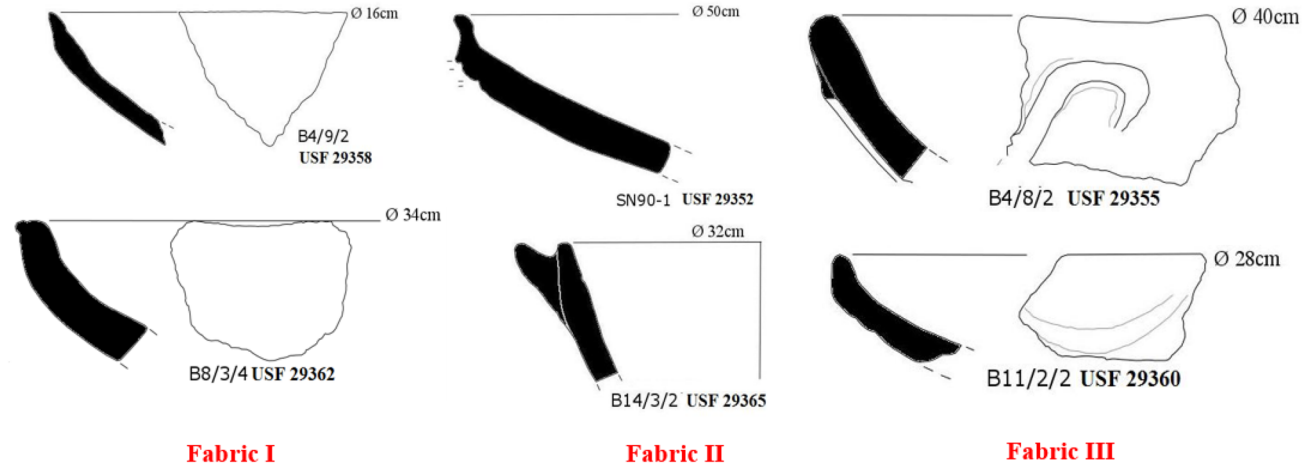

Fig. 5 Cup typologies belonging to fabrics I, II, III

Table 3 List of the samples with indication of the analytical techniques applied (petrographic examination of thin sections, portable X-ray fluorescence spectrometry, electron microprobe analysis)

Sample ID	Fabric	Petrographic analysis	PXRF	EPMA
USF29349	I		×	×
USF29350		×	×	
USF29351	II	×	×	
USF29352			×	×
USF29353			×	×
USF29354	III	×	×	
USF29355		×	×	
USF29357		×	×	
USF29358		×	×	
USF29359		×	×	
USF29360		×	×	
USF29361	IV	×	×	
USF29362		×	×	
USF29363		×	×	
USF29364			×	×
USF29365		×	×	
USF29366			×	×
USF29367	V		×	×
USF29368		×	×	
USF29369		×	×	
USF29370		×	×	
USF29371			×	×
USF29372	VI		×	×
USF29373			×	×
USF29374			×	×
USF29375	Adobe		×	×
USF29376	Cooking plates	×	×	
USF29377		×	×	
USF29378			×	×

The instrument was placed in an upright position on a plastic stand with samples balanced on top. Three readings of 120 s each were taken for each sherd over the edge, inner, and outer surfaces with a beam area of 5 × 7 mm. Flat areas on the specimens' surface were chosen to reach the instrument's maximum potential, after following a two-cycle cleaning procedure involving washing and then scrubbing the samples' surface with a very fine abrasive paper. Raw data for each of the trace elements were obtained using Excel software that incorporates values for 40 standards tested with the instrument. To evaluate the consistency of each trace element and to interpret the geochemical data in accordance with established analytical conventions efficiently (Emmitt et al. 2018; Forster et al. 2011; Hunt and Speakman 2015; Karacic and Osborne 2016; Newlander et al. 2015), the three measurements taken on each sherd were averaged, and then transformed using base log 10.

The resulting statistical analysis combined principal components analysis (PCA) and Euclidean distance hierarchical clustering. pXRF has been increasingly utilized in non-destructive archeological research for a variety of projects (Karacic and Osborne 2016; McKendry 2015; Mommsen 2004; Neff 2002; Stovel et al. 2016; Tanasi et al. 2017). It was chosen for this study for several reasons: since it requires minimal sample preparation, it is relatively inexpensive, and the data it generates can potentially be used to differentiate between ceramics with different elemental compositions in a relatively short amount of time. Overall, most of the elements which are of interest for compositional analysis of archeological ceramics can be obtained accurately and precisely by pXRF (Emmitt et al. 2018; Forster et al. 2011; Hunt and Speakman 2015; Newlander et al. 2015; Tykot 2016). To potentially distinguish among different groups of ceramics, Rb, Sr, Y, Zr, and Nb were selected for the analysis.

4.3 Chemical analysis using an electron microprobe (EPMA)

To enhance the interpretation of more problematic samples, 12 specimens (USF29349, 29352, 29353, 29364, 29366, 29367, 29371, 29372, 29373, 29374, 29375, 29378) were analyzed with an EPMA JEOL 8900R Superprobe, equipped with a wavelength-dispersive spectrometer, at the Florida Center for Analytical Electron Microscopy at the Earth and Environment Department of the Florida International University of Miami, and according to standardized procedures proposed by Malainey (2011). Electron probe microanalysis (EPMA) was performed on the clayey matrix. This method of analysis can help to either confirm or exclude suspected rocks as sources of raw materials by detecting phases < 15–20 µm, including minerals such as feldspars, micas and quartz, which are relevant for the identification of the technological condition of firing and the clay's properties (Cultrone et al. 2001; Cuomo di Caprio 2007). The possibility to combine backscattered electron (BSE) images, and secondary electron (SE) images, without destroying the samples, offers a solid basis for integrated interpretations of the ancient ceramics. The precise compositional and fabric features resulting from EPMA are overall indicators of raw materials and their provenance, and even of occurring technological constraints, such as firing temperature and atmosphere.

5 Results

5.1 Petrographic data

The analysis of the 17 thin sections was carried out following Whitbread's classification (1989). Such an approach allowed the characterization of the entire group of samples into petro-groups, or fabrics, according to the occurrence of different features within the clay paste. Samples' mineral and textural features, such as grains' distribution, optical activity, angularity, porosity, and clay matrix, have been described to detect the use of different clay sources, or a specific production recipe, thus highlighting the practice in use for the pottery from the hill of Sant'Ippolito during the Middle Bronze Age. Samples 29355 (cup), 29360 (cup), and 29370 (cooking pan) were not included in the petrographic analysis due to the poor preservation of their texture after the treatment. According to the petrographic analysis, two different fabrics can be distinguished: SIP1 and SIP2. On the basis of groundmass texture and temper, SIP1 can be further divided into two sub-groups, SIP1a and SIP1b.

Fabric SIP 1a (Fig. 6, Table 4) includes samples 29354 (cup), 29361 (situla), 29376 (hot-plate), and it is characterized by a semi-fine light brown groundmass. The coarse fraction is mainly composed by poorly sorted grog, and frequent microfossils, while the fine fraction is characterized by very fine quartz particles, and rare vitrified grains.

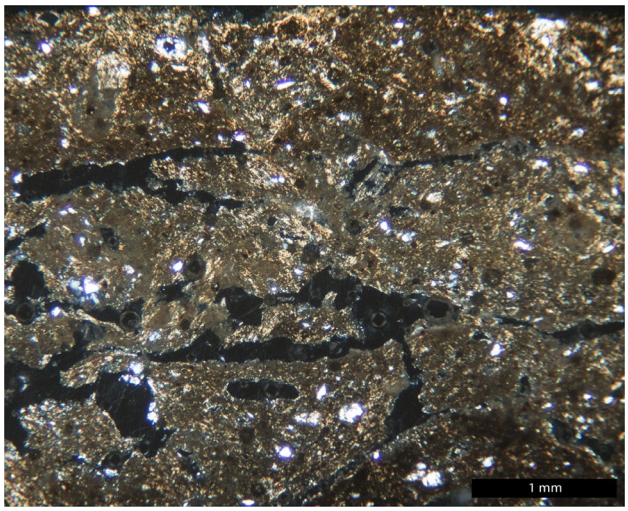

Fig. 6 Fabric SP1a: thin section of sample USF29354 (B4/7/6) XP (×40)

Fabric SIP1b (Fig. 7, Table 5) includes samples 29350 (foot), 29363 (cooking pan), 29368 (cooking pan), 29369 (cooking pan), and it is characterized by a semi-fine light brown groundmass. The coarse fraction is mainly composed by moderately sorted grog and no microfossils, while the finer fraction is mainly quartz.

Overall, the SIP1 group, including both SIP1a and SIP1b, is characterized by very porous and micritic clay containing both sedimentary and intrusive rocks. The temper is overall composed by clasts of sedimentary rocks, grog, and microfossils, which are very common in the geological unit around Mt. Etna and in eastern Sicily (Barone et al. 2012; Basilone 2018; Rodriguez et al. 2015). Group SIP1a differs on average from group SIP1b mainly because of the lack of abundant fossils among samples of the latter, most likely coming from micrite carbonates.

Fabric SIP2 (Fig. 8, Table 6) includes samples 29351, 29357, 29358, 29359, 29362, 29365, 29377, and it is characterized by a coarse and semi-fine dark and very dark brown texture, composed mainly by grog and fossiliferous groundmass.

This petrographic group is characterized by the presence of a coarse fossiliferous clay, whose temper can be described as mainly composed of homogeneous microfossils, high amounts of grog and secondary grog, and fine silicate grains. Its overall texture is more porous than SIP1, and inclusions are randomly distributed across the thin sections, with a much higher presence of microfossils and small silica grains.

Table 4 Petrographic description of fabric SIP1a

Microstructure	The microstructure shows meso-voids, common micro- to meso-channels, and very few common meso-vughs. They are all elongated, usually open spaced, and show parallel orientation with vessel margins, although some have different orientation even within the same sample. Rarely, voids show secondary calcification on the inner edges.
Groundmass	The groundmass is slightly active and fairly homogeneous across the thin section both in PPL and XP, with few slight changes in color from brown to very light brown (x 40).
Inclusions	Coarse:fine:voids (c:f:v) 35:40:25 Coarse fraction = from 2 to 0.25 mm Fine fraction = from 0.25 to 0.01 mm The inclusions all have different sizes (polymodal distribution). The coarse fraction is characterized by poorly sorted and heterogeneous grog, and few microfossils (foraminifera and globigerina). The fine fraction is moderately sorted, medium to fine calcite particles and medium sand to fine silt size, sub-angular in shape, and homogenously distributed.
Coarse fraction	Dominant: grog, which has been identified as 0.25–2 mm sub-angular and elongated clasts, attested in two different types. One is a dark brown-black, mostly opaque, slightly optically inactive type, usually containing coarser quartz particles and very few microfossils. The other one is a lighter brown, mostly opaque, and optically inactive type that is characterized by the presence of finer silica grains. Within some of the microfossils' bodies, secondary deposition processes and oxidization can be found. Frequent: microfossils, such as foraminifera and globigerina, and bivalves, ranging between 1 and 0.5 mm in size; secondary grog attested as 0.25–0.7-mm clasts.
Fine fraction	Dominant: very coarse quartzite clasts, heterogeneously distributed along the section, sub-angular in shape, ranging from 0.25 to 0.1 mm. Rare: biotite mica and vitrified groundmass.

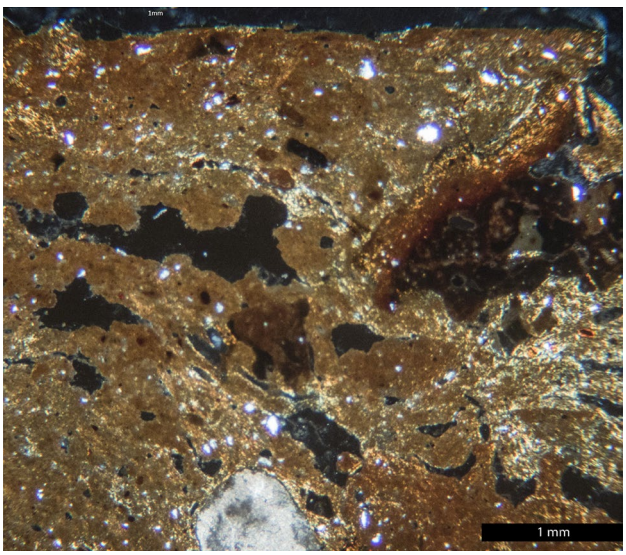

Fig. 7 Fabric SP1b: thin section of sample USF29369 (SN2) XP (×40)

5.2 Chemical analyses

5.2.1 pXRF

The results of the chemical analysis carried out over the entire ceramic assemblage (= 29) showed the occurrence of a significant range for Sr, Zr and Rb, while the range is small for Y and Nb. However, an overall homogeneity among Rb, Sr, Y, Zr, and Nb values is still noticeable. Elements such as Sr, Zr and Rb are among the most meaningful trace elements for discriminating between groups of compositionally different samples, and it seems that variations occurring among those elements also proportionally affect the content of both Y and Nb. However, the same elements do not seem to consistently affect one another (Table 7).

Some noticeable variations are present for sample 29353, which shows the highest concentration of Sr (5497 ppm), and very high concentrations of Y (28), Zr (178), and Nb (19). Sr concentrations for samples 29372 (4086) and 29375 (2019) are among the highest recorded. However, the latter represents a very interesting specimen, since it also bears the lowest amount for Rb (60), Y (16), Zr (88), and Nb (10). This sample is a fragment of the adobe found on the ground floor of the hut. Minor compositional variations affect sample 29349, which bears one among the lowest concentrations of Rb (83) and Nb (17), and very high values for Sr (1740) and Zr (203). The lowest Sr concentration (706) has been recorded for sample 29374, which is also characterized, on the other hand, by the highest Zr concentration (228) among the entire group of samples. Other meaningful variations have been recorded for Rb concentrations among samples 29364 (73), 29366 (77), and 29373 (79). Sample 29364 also bears a very low concentration of Nb (16). Rb values are low among the samples 29372 (83) and 29373 (79), which also show very low concentrations of Y (21). Table 8 includes the ppm values recorded for all the samples included in this study.

What is important, however, is the interpretation of the further statistical analysis, which provides clues about elements' load for each sample. For this reason, principal components analysis was performed using a variance–covariance relation, due to samples' overall high homogeneity (Fig. 9).

Table 5 Petrographic description of fabric SIP1b

Microstructure	The microstructure shows common planar and sub-rounded meso-voids and -channels. Macro-voids and vughs are very rare. They are all commonly elongated, single spaced, and rarely parallel with vessel margins. Frequently, some voids across the thin section show secondary calcification on the inner edges.
Groundmass	The groundmass is, like SIP1a, slightly active and homogeneous across the thin section both in PPL and XP (x 40), but less porous than its counterparts.
Inclusions	Coarse:fine:voids (c:f:v) 20:65:15 Coarse fraction = from 1.5 to 0.25 mm Fine fraction = from 0.25 to 0.02 mm The inclusions have a polymodal distribution, with the coarser fraction being moderately sorted and randomly oriented. It is characterized by mostly heterogeneous grog and big calcite grains. The fine fraction is moderately sorted, mostly medium to fine calcite and quartzite particles, sub-angular in shape, and homogenously distributed.
Coarse fraction	Dominant: grog ranging between 1.5 and 0.25 mm, usually in the shape of sub-angular and elongated clasts, which have been attested both as dark brown-black and light brown type, mostly opaque, slightly active and containing mostly quartz. Rare: calcite clast and quartz crystal bigger than 1 mm.
Fine fraction	Dominant: very coarse quartzite clasts, homogeneously distributed along the section, sub-angular in shape, ranging from 0.25 mm and 0.02 mm in size. Rare: vitrified particles.

The scatter plot for principal components 1 and 2, which accounts for more than 95% of the cumulative variation among variables, clearly shows one main group of 24 specimens clustered altogether, including all the samples regardless of their shape, function, and fabric detected. Three major outliers (29353, 29372, 29375) are, instead, plotted separately far from the main group. These samples are strongly characterized by an overall anomalous content of Sr, Zr, and Y in relation to all the other specimens, and to one another, and they consistently differ from the main cluster. Other minor outliers, as they are plotted closer to the main cluster than the major outliers, are samples 29349 and 29374. PCA loadings for PCA1 suggest Sr is the main trace element driving the resulting distinction between different compositional groups of samples, while Rb and Zr play the major role for PCA2. Variations occurring among Zr concentration, however, are not able to discriminate among groups by itself, and its loading can be understood only in regard to Sr concentration. The hierarchical cluster, computed according to Euclidean distance (Fig. 10), further confirms what PCA analysis previously suggested, as it displays the samples 29372 and 29353 in the top right of the graph lacking any immediate links with their compositionally neighboring counterparts, including a minor outlier (29374). The adobe fragment is, instead, displayed closer to the other minor outlier (sample 29349) in the top left, thus showing how these two groups differ compositionally.

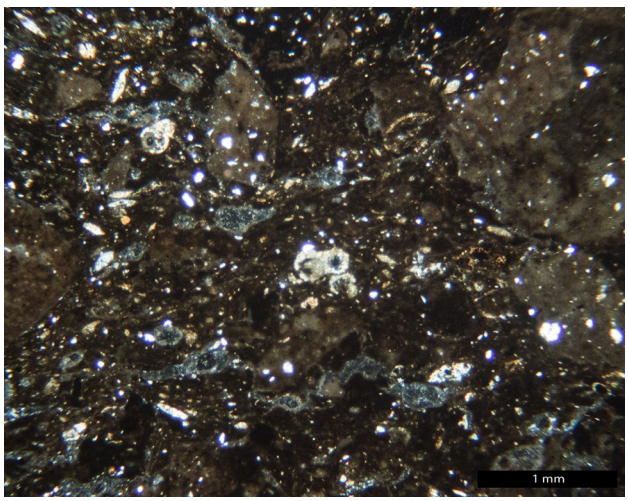

Fig. 8 Fabric SIP2: thin section of sample USF29359 (B4/14/4) XP (×40)

5.2.2 EPMA

The analysis of 12 samples by microprobe aimed at investigating their ambiguous chemical signature detected via pXRF, in relation to the entire ceramic assemblage. Although this method concerns the petrographic assessment of the samples, it also provides important clues in regard to their chemical composition. Such an approach, therefore, allowed the further characterization of the selected samples into different groups according to differences among the peaks detected for Si, Fe, and Ca.

Samples were obtained following the same procedures previously adopted for the optical analysis, and later on treated to make them suitable for the microprobe analysis by applying a very thin layer of gold on the sections' surface. According to the results, the samples showed, on average, very similar chemical signatures. Slight differences have been detected among samples' main clay components (Al, Si, Fe), although this result, per se, is not really indicative for the definition of specific production features. However, the quantitative variation between these elements among the group of samples has highlighted

Table 6 Petrographic description of fabric SIP2

Microstructure	The microstructure is characterized by common voids, usually in the shape of meso-voids and -channels. On average they are planar, although more complex shapes, including rounded and sub-rounded, have also been detected, and they have long axis orientation parallel with margins and oblique. They are single and open spaced.
Groundmass	The groundmass looks fairly homogeneous and very porous, on average highly active compared to SIP1 (a–b). The color does not vary much switching from XP to PPL (x 40), showing very similar shades of dark brown.
Inclusions	Coarse:fine:voids (c:f:v) 60:20:20 Coarse fraction = from 2 to 0.4 mm Fine fraction = from 0.4 to 0.01 mm The inclusions have polymodal distribution. The coarser fraction is poorly sorted and on average randomly distributed, although big grains sometimes show oblique orientation. It is mainly composed of grog and microfossils, along with calcite and silica grains. The fine fraction is mainly characterized by sub-angular silica particles.
Coarse fraction	Dominant: grog ranging between 2 and 0.2 mm, usually in the shape of sub-angular and elongated clasts, which have been attested both as dark brown-black and light brown type, mostly opaque, optically active and containing mostly quartz and microfossils (bivalves and foraminifera). Secondary grog is also present (between 1 and 0.4 mm). Microfossils (foraminifera and globigerina) ranging between 0.7 and 0.4 mm are also abundant. Rare: calcite clast and quartz grains (.5–0.4 mm)
Fine fraction	Dominant: very coarse quartzite clasts, heterogeneously distributed along the section, sub-angular in shape, ranging from 0.4 to 0.02 mm in size. Frequent: calcite particles and microfossils (bivalve), along with silica grains less than 0.4 mm.

Table 7 Descriptive statistics of the total (=29) ceramic assemblage

	Min	Max	Mean	Std. dev.
Rb	60	114	94	12
Sr	706	5497	1477	976
Y	16	30	25	3
Zr	88	228	173	21
Nb	10	25	19	3

interesting compositional patterns, which might be useful for the resulting distinction between groups of fabrics. Two main groups can be distinguished: Group A and Group B.

Group A (Fig. 11), consisting of five samples (29349, 29352, 29353, 29364, 29378), was detected according to the association between high amounts of Al, Si, and Ca and low Fe content. The digital image (×40) shows a slightly porous clay matrix with meso- and macro-vughs, which likely suggests the use of degradable compounds added as temper. The upper foot fragment (29353) that has been considered an outlier shares such features.

Group B (Figs. 12, 13) counts five samples with low amounts of Al, Si, and Ca, always associated with higher Fe content (29367, 28371, 29372, 29373, 9374). All the samples in this group showed very similar composition, thus suggesting they were more likely to have been made with closely related raw materials. Interestingly, all the *pithoi* are compositionally related to two cooking pans (29367, 29371). Besides, the presence of sub-rounded meso-vughs, the matrix of these groups show, on average, the highest degree of compactness, which further confirms the importance of making these types more resistant to eventual shocks.

Table 8 pXRF results for trace elements, with values reported as ppm values

Sample ID	Rb	Sr	Y	Zr	Nb
29349	83	1740	26	203	17
29350	99	939	27	171	22
29351	96	1614	25	181	22
29352	106	1261	29	173	19
29353	88	5497	28	178	19
29354	96	1274	27	170	23
29355	103	997	28	180	21
29357	90	1459	25	170	20
29358	103	1449	24	180	21
29359	95	1357	26	172	19
29360	98	972	25	169	21
29361	97	1321	28	176	19
29362	99	1377	27	183	21
29363	95	1062	25	171	19
29364	73	1305	21	175	16
29365	84	1087	26	188	19
29366	77	1134	23	169	19
29367	105	1095	30	172	20
29368	114	1025	29	177	22
29369	107	974	26	174	20
29370	103	1281	26	185	25
29371	105	862	23	170	19
29372	83	4086	21	160	18
29373	79	1162	21	159	20
29374	89	706	25	228	20
29375	60	2019	16	88	10
29376	100	1263	27	172	21
29377	105	1083	27	174	19
29378	83	1424	21	157	16

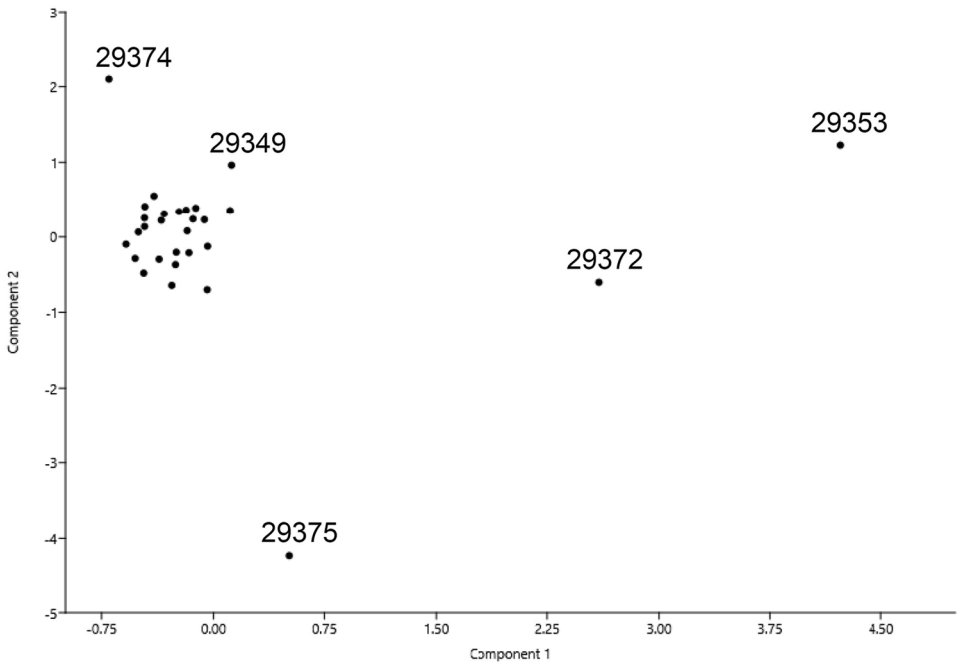

Fig. 9 Biplot of the two principal components (PCA) showing all the samples analyzed for this study

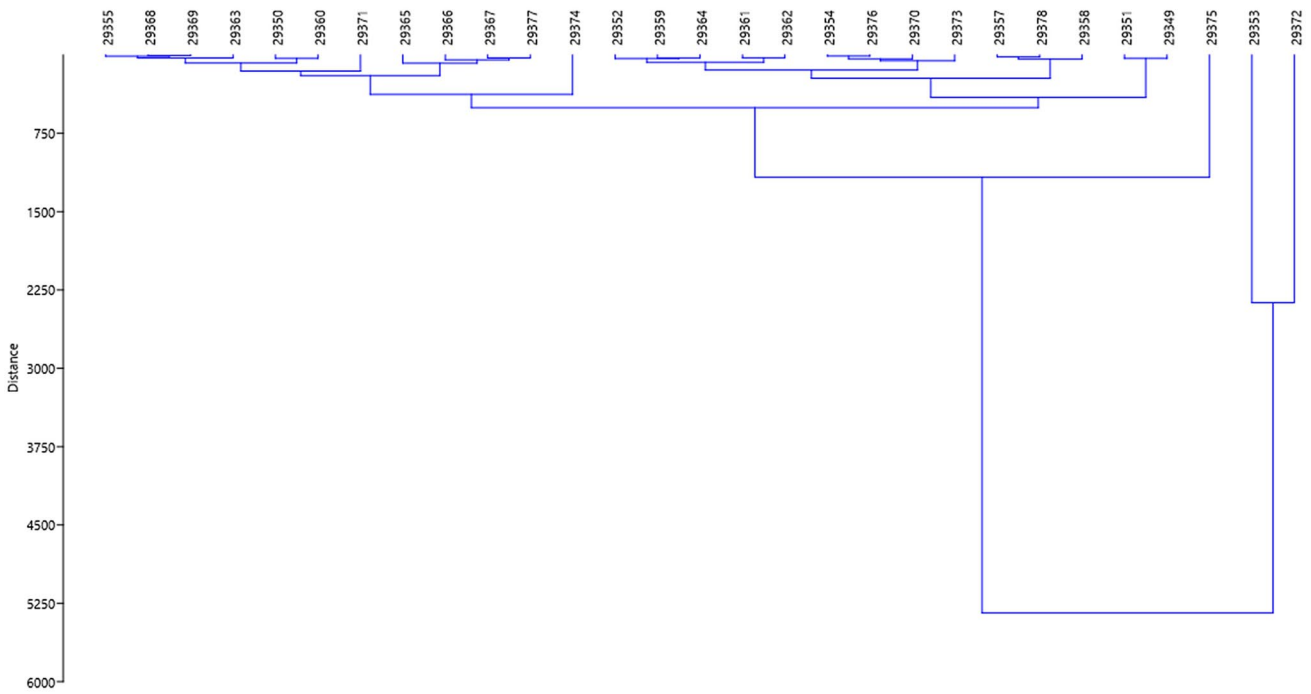

Fig. 10 Euclidean distance of the entire group of samples for trace elements (Rb, Sr, Y, Zr, Nb)

Besides, these two main groups minor compositional variations occur among two samples (29366, 29375), although they do not seem to share any compositional pattern with one another to the extent that they be considered as a group apart. It is important to remember that sample 29375 is adobe and it was also identified as an outlier by the pXRF analysis.

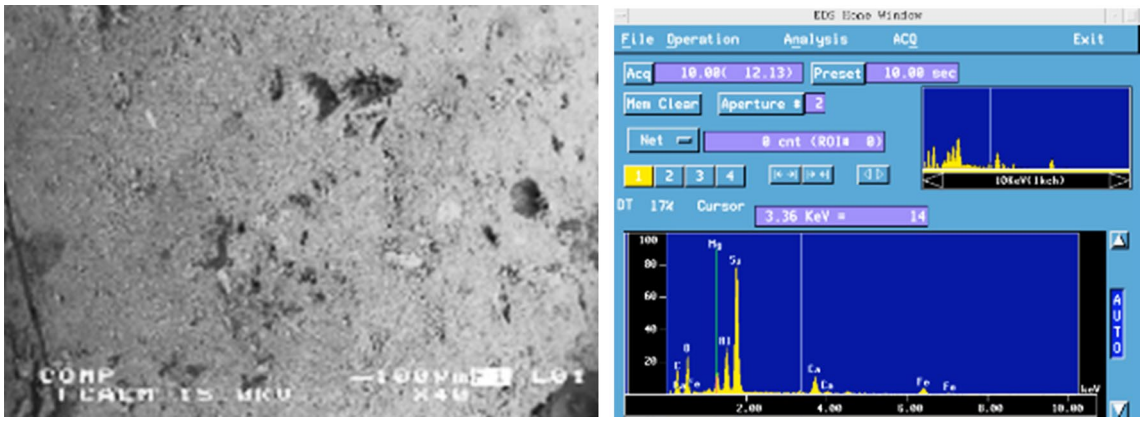

Fig. 11 Group A: backscattered electron image (×40) 100 µm and spectrum indicating peaks for Al, Si, Ca and Fe (sample USF 29378—B5/4/SIP4). The picture shows heterogenous voids that follow a specific pattern, thus suggesting the use of a higher concentration of organic matter as temper, which disappeared after the firing process and, then, left voids behind within the matrix

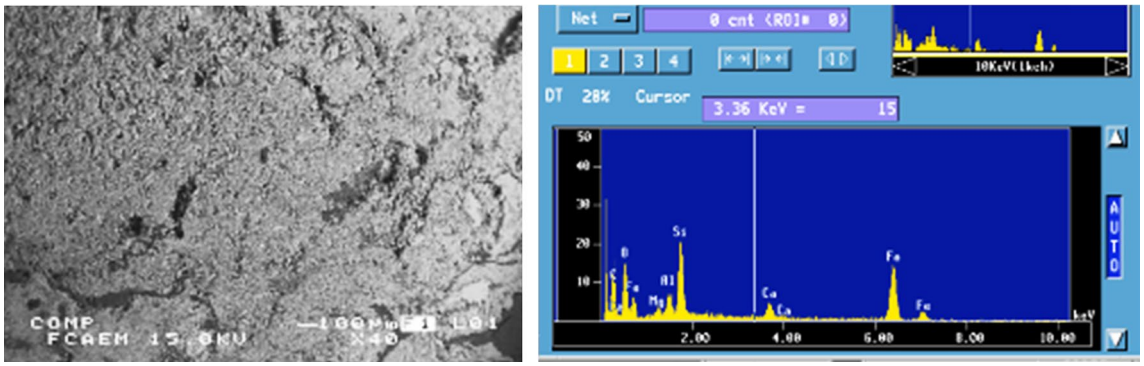

Fig. 12 Group B: backscattered electron image (×40) 100 µm and spectrum indicating peaks for Al, Si, Ca and Fe (sample USF 29372—B4/7)

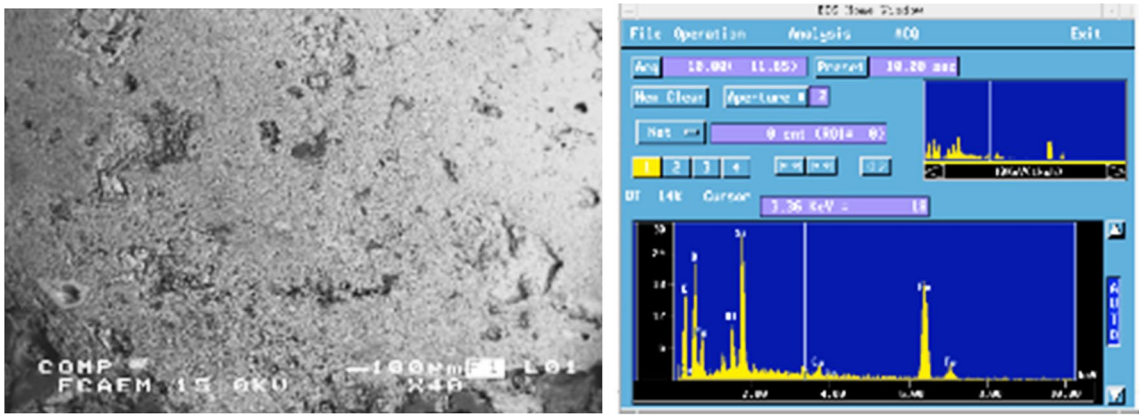

Fig. 13 Group B: backscattered electron image (×40) 100 µm and spectrum indicating peaks for Al, Si, Ca and Fe (sample USF 29373—B13/14/7)

6 Discussion

The findings from the application of the three analytical techniques have provided significant new data to expand the discussion on the significance of the evidence from the site of St. Ippolito (Table 9).

With respect to the outcomes of the petrographic analysis, the Thapsos pottery samples from Area B at the hill of Sant'Ippolito show a relative homogeneity of production, characterized by the use of fossiliferous clay tempered mainly with grog, additional carbonate and siliceous rocks, probably related to the geological setting of the hill itself (Barone et al. 2012; Basilone 2018; Rodriguez et al. 2015). Intrusive rocks are far less abundant.

The most interesting aspect of the petrographic study is the recognition of specific "pottery recipes" for both tableware (SIP1a and SIP2) and cooking ware (SIP1b). The use of finer and less porous clays for SIP1b, characterized by low carbonate concentrations, absence of microfossils, and high concentration of silica particles, may be related to the choice of the potter to enhance the resistance of this class to thermal shocks occurring during the firing stage. This interpretation is further supported by the optical inactivity of the samples from this fabric across the sections, which highlights even more interesting clues in regard to the choices made by ancient potters. The light brown color, which is distinctive for this fabric, may suggest the occurrence of a setting that supposedly could reach very high temperatures (> 900 °C), causing the vitrification of finer minerals across the sections. The combination of these features also suggests that the firing more likely occurred within a kiln, rather than in a firing pit, since reaching higher temperatures commonly requires skills for controlling the fire and the atmosphere.

On the other hand, the abundance of fossils and different types of carbonate rock-based tempers and grog suggests a different approach to the firing strategy for this class. Here, the combination between the dark color in the matrix and the presence of microfossils is linked to the reduced atmosphere setting. This triggers the occurrence of choices made by potters to eliminate the risk of fractures, since the formation of calcium oxide creates a significant stress in the pottery (between 650 and 898 °C) and, thus, it may generate cracks in the ceramic body (Barone et al. 2012; Borgna and Levi 2015; Cuomo di Caprio 2007; Quinn 2013; Veca 2015). Although such features cannot be clearly confirmed at this stage due to the lack of any assessment about the crystallographic properties of the minerals detected among these samples, the results may provide important clues in regard to technology. Therefore, this class of pottery may have been fired differently, and at different temperatures, than the former one, perhaps according to constrains derived from the nature of the clays in use and the skills kept by potters. The lack of organic matter among all the fabrics can be also addressed as further confirmation for the idea that both types were fired at temperatures above 700 °C, either in a kiln or in a firing pit. This information is crucial because it highlights the importance of petrography as a necessary tool that cannot be excluded from the study and the interpretation of ceramic artifacts, especially to understand the evolution of ancient technology (Levi and Muntoni 2014; Mommsen 2004; Quinn 2013; Santacreu 2014; Veca 2014b; Whitbread 1989).

The compositional results of the Thapsos ceramic assemblage also revealed an overall homogeneity. The pXRF provided precious clues for the understanding of the compositional proximity among the specimens. Some of the micro-variations detected among the elements might be the result of the overall high presence of grog within each sample, which might potentially affect the overall analysis by

Table 9 List of the samples with the indications of the results from the three analytical approaches

Sample ID	Autoptic fabric	Petrographic fabric	PXRF	Microprobe
USF29349	I		×	Group A
USF29350		SIP 1B	×	
USF29351	II	SIP 2	×	
USF29352			×	Group A
USF29353			×	Group A
USF29354	III	SIP 1A	×	
USF29355		–	×	–
USF29357		SIP 2	×	
USF29358		SIP 2	×	
USF29359		SIP 2	×	
USF29360		SIP 2	×	
USF29361	IV	SIP 1A	×	
USF29362		SIP 2	×	
USF29363		SIP 1B	×	
USF29364			×	Group A
USF29365		SIP 2	×	
USF29366		–	×	–
USF29367	V		×	Group B
USF29368		SIP 1B	×	
USF29369		SIP 1B	×	
USF29370		–	×	–
USF29371			×	Group B
USF29372	VI		×	Group B
USF29373			×	Group B
USF29374			×	Group B
USF29375	Adobe	–	×	–
USF29376	Cooking plates	SIP 1A	×	
USF29377		SIP 2	×	
USF29378			×	Group A

pXRF due to the width of its beam (Hunt and Speakman 2015; Tykot 2016). Nonetheless, the samples were made according to very close manufacturing strategies, as the detected chemical homogeneity demonstrates.

The PCA suggests the occurrence of three outliers, specifically an upper foot cup (29353), a storage jar (29372), and the adobe fragment (29375). The cup represents an interesting case, considering its typological relation with the tableware types we encountered during this study. It is noticeable that its values (highest Sr and Zr concentrations, and lowest Y content) are slightly off from the overall picture of the dataset. Unfortunately, no clay source had been investigated at the time of the recovery, and the artifacts cannot be properly correlated to any of the nearby clay sources at this stage, which we aim to accomplish in the future. Further investigations might provide the proper data to understand additional clues in regard to procurement strategies, given also the occurrence of an adobe fragment (29375) among the detected outliers. The other outlier consisted of a storage jar (29372). The likelihood for the *pithos* to be considered a common specimen is very low. According to the nature of the archeological evidence, the location of the site, and the context of the ceramic assemblage, it is more likely that the *pithos* was manufactured differently, perhaps from a different workshop or with a different recipe than those that overall produced the repertoire here investigated. The sample 29374, clustered in a different reference group than the major one, further confirms this hypothesis. The complex debate concerning the movement of big storage jars across the landscape might provide precious insights, whether they were the material product of a larger *koine* of potters or a privileged specialization for specific socio-political agents within the broader prehistoric political network (Alberti 2013; Doonan 2001; Raneri et al. 2015a; Tanasi 2010b; Veca 2014a, b, 2015). The computation of the Euclidean distance served as a further confirmation that the petrographic fabrics and the chemical composition could match. Among all the samples, groups according to the classification resulting from the petrographic assessment are also chemically distinguishable. The overall occurrence of more or less fossiliferous clays, along with the use of siliceous- and carbonate rock-based tempers, may be related to specific choices made among potters and to the diversification of their recipes among workshops (Buxeda i Garrigos et al. 2001; Quinn and Day 2007; Santacreu 2014; Stovel et al. 2016; Whitbread 1986). However, at this stage, it is too early to address how extensive was the network that made the potters choose specific recipes, given how little we know about clay sources, workshops, and settlement networks throughout this area during the Middle Bronze Age. PXRF was very useful in combination with the petrographic methods, which helped at defining groups of artifacts that can be distinguished within the broader and chemically homogeneous ceramic assemblage.

Furthermore, PCA clearly showed how the samples 29349 and 29374 form a compositionally distinguished group from the main group of Thapsos ceramics. 29349 represents an early North Pantalica specimen, proving that the well-known cultural discontinuity occurring between the two pottery traditions was not just with respect to style and shape repertoire, but it perhaps affected clay procurement and manufacturing strategies (Tanasi 2008). Also remarkable is the proximity between this sample and one of the three *pithoi* (29374) analyzed, which further confirms the assumption that some specific types here represented could have been produced somewhere else in relation to the entire assemblage. The resulting data are precious clues that will provide additional pieces to the broader understanding of the Middle Bronze Age of Sicily.

These assumptions become clearer with the inclusion of the results coming from the compositional study via EPMA of a selected group of samples. Although the samples on average confirm a high compositional homogeneity, they were classified into two distinctive groups of samples according to differences in the clayey matrixes that are either high in Ca (A) or Fe (B). The results highlight the possibility that some recipes required a mixture of clays according to potters practices and functionality. Yet, understanding the provenance and the relation among each production type and clay source cannot be fully discerned. Within Group A, higher Ca concentrations among samples of the tableware group, (29349, 29352, 29353), one of the coarse group (29364), and a coarse cooking plate (29378), might suggest the use of highly fossiliferous clays, and the use of carbonate rocks added as temper. Such an interpretation strengthens the previous petrographic assessment. Samples within Group B, which are functionally related to cooking pans (29367, 29371) and storage jars (29372, 29373, 29374), show very high concentrations of Fe that are always associated with very low levels of Ca, thus triggering the use of clays lower in fossiliferous content, along with the use of less carbonate rocks as temper, than Group A. The distinctive association between Ca and Fe concentrations within the ceramic groups is here interpreted as a marker for the identification of two distinct clay pastes that are characterized either by clays higher in Fe or in Ca content. However, whether this difference is the result of specific choices made by potters or imposed by the availability of local raw sources still represents a deficiency within the broader understanding of local ceramic production.

Finally, the presence of the two North Pantalica samples 29349 and 29364 in the same Group, already grouped together by pXRF in a cluster apart, further reinforces the hypothesis of a discontinuity in the manufacturing processes between the Thapsos (MBA) and North Pantalica (LBA) types.

7 Conclusions

The results of the archeometric analyses testify to a petrographic and chemical homogeneity for Thapsos pottery production at the site of St. Ippolito. Comparing the petrographic data with those previously presented on the materials from Monte San Paolillo di Catania and Grotte di Marineo di Licodia Eubea, it is now possible to draw some preliminary conclusions on the manufacturing strategies and traditions of the Etnean territory spanning from the Southeastern slope of the Etna volcano and the eastern side of the Hyblaean plateau. The discriminating petrographic characteristic between the three productions is the occurrence of volcanic inclusions (rocks, glass, plagioclase, pyroxenes), largely attested at Monte San Paolillo di Catania and Grotte di Marineo di Licodia Eubea and basically absent at St. Ippolito.

On the other hand, the only fabric without volcanic materials observed at Grotte di Marineo (fabric A: Tanasi 2015, p. 56) shares same petrographic features of SIP 1A and SIP 2, such as limestone inclusions and fossiliferous groundmass. The use of grog and microfossils and limestone inclusions also seems to be another feature in common between the production of Grotte di Marineo and St. Ippolito.

In this perspective, the use of volcanic tempers becomes the principal indicator of the Etnean production of Thapsos pottery. The different evidence offered by St. Ippolito shows how such a site should be considered as part of another technological *koine*, characterized by different manufacturing strategies. Considering that the territory of Caltagirone is closer to the geographical district of Siracusa than to that of Catania, it is not inappropriate to suggest that Thapsos potters at St. Ippolito shared the same technological knowledge of those from Siracusa. However, the lack of archeometric data for the Thapsos pottery from the Megarian and Siracusan district leaves the problem open still, but a gap that we plan to bridge by extending the archeometric survey to Thapsos ceramic assemblages from that area.

Acknowledgements Authors are grateful to Dr. Domenico Amoroso, former director of Musei Civici 'Luigi Sturzo' di Caltagirone and field director of the excavation carried out at Sant'Ippolto hill, whose results are in part subject of the present article, for his trust and support in the development of the research.

Compliance with ethical standards

Conflict of interest The authors declare that they have no conflict of interest.

Ethical approval This article does not contain any studies with human participants or animals performed by any of the authors.

Informed consent Informed consent was obtained from all individual participants included in the study.

References

Alberti G (2004) Contributo alla seriazione delle necropoli siracusane. In: La Rosa V (ed) Presenze micenee nel territorio siracusano. Aldo Ausilio Editore, Padova, pp 99–170

Alberti G (2008) La ceramica eoliana della facies del Milazzese: studio crono-tipologico e culturale sulla base dei dati editi da Filicudi, Panarea, Salina. BAR Publishing, Lipari

Alberti G (2013) A Bayesian ^{14}C chronology of Early and Middle Bronze Age in Sicily. Towards an independent absolute dating. J Archaeol Sci 40:2502–2514

Alberti G (2017) New light on old data: toward understanding settlement and social organization in Middle Bronze Age Aeolian Islands (Sicily) through quantitative and multivariate analysis. J Archaeol Sci Rep 11:310–329

Amoroso D (1987) Una testimonianza di viabilità preistorica: la strada delle tombe nella necropoli della Montagna di Caltagirone. In: Atti del III Convegno di Studi sulla viabilità antica in Sicilia, pp 15–22

Barone G, Crupi V, Longo F, Majolino D, Mazzoleni P, Tanasi D, Venuti V (2011a) FT-IR spectroscopic analysis to study the firing processes of prehistoric ceramics. J Mol Struct 993:147–150

Barone G, Mazzoleni P, Tanasi D, Veca C (2011b) La tecnologia della produzione ceramica nel Bronzo Medio siciliano: il caso dei pithoi di Monte San Paolillo (Catania). Rivista di Scienze Preistoriche LXI:175–198

Barone G, Mazzoleni P, Patanè A, Tanasi D (2012) Analisi petrografiche e geochimiche su ceramiche siciliane dell'età del Bronzo Medio: il sito di Licodia Eubea. In: VI Congresso Nazionale di Archeometria "Scienza e Beni Culturali", Pavia, 15–18 Febbraio 2010

Basilone L (2018) Lithostratigraphy of Sicily. Springer, Cham

Bietti Sestieri AM (2015) Sicily in Mediterranean history in the Second Millennium BC. In: Van Dommelen P, Knapp B (eds) The Cambridge prehistory of the Bronze and Iron Age Mediterranean. Cambridge University Press, Cambridge, pp 74–95

Borgna E, Levi ST (2015) The Italo-Mycenaean connection: some considerations on the technological transfer in the field of pottery production. In The transmission of technical knowledge in the production of ancient Mediterranean pottery, proceedings of the international conference at the Austrian archaeological institute at Athens, 23rd–25th November 2012, pp 115–139

Buxeda i Garrigos J, Kilikoglou V, Day PM (2001) Chemical and mineralogical alteration of ceramics from a Late Bronze Age kiln at Kommos, Crete: the effect on the formation of a reference group. Archaeometry 43:187–198

Caso G, Tanasi D, Tykot RH (2017) Beyond typology: archaeometric characterization of Sicilian Middle Bronze Age ceramics, archaeological institute of America 118th annual meeting abstracts, pp 40–72

Crispino A, Ippolito S (2014) Caltagirone: nuovi dati sull'abitato dagli scavi Orsi. Rivista di Scienze Preistoriche LXIV:115–149

Cultrone G, Rodriguez-Navarro C, Sebastian E, Cazalla O, De la Torre MJ (2001) Carbonate and silicate phase reactions during ceramic firing. Eur J Miner 13:621–634

Cuomo di Caprio N (2007) La ceramica in archeologia 2: antiche tecniche di lavorazione e moderni metodi di indagine. L'Erma di Bretschneider, Roma

Doonan O (2001) Domestic architecture and settlement planning in Early and Middle Bronze Age Sicily: thoughts on innovation and social process. J Mediterr Archaeol 14(2):159–188

Emmitt JJ, McAlister AJ, Phillipps RS, Holdaway SJ (2018) Sourcing without sources: measuring ceramic variability with pXRF. J Archaeol Sci Rep 17:422–432

Forster N, Grave P, Vickery N, Kealhofer L (2011) Non-destructive analysis using pXRF: methodology and application to archaeological ceramics. X-Ray Spectrom 40(5):389–398

Hunt AMW, Speakman RJ (2015) Portable XRF analysis of archaeological sediments and ceramics. J Archaeol Sci 53:1–13

Jones R, Levi ST, Bettelli M, Vagnetti IL (2014) In: lberti L (ed) Mycenaean pottery: the archaeological and archaeometric dimensions. Instituto di Studi sulle Civilta' Italiche e del Mediterraneo Antico, Roma

Karacic S, Osborne JF (2016) Eastern Mediterranean economic exchange during the Iron Age: portable X-ray fluorescence and neutron activation analysis of cypriot-style pottery in the Amuq valley, Turkey. PLoS One 11(11):1–17

Levi ST, Muntoni IM (2014) L'archeometria della ceramica in Italia: storia degli studi, risultati e prospettive della ricerca. In: Studi di Preistoria e Protostoria: 150 anni di preistoria e protostoria in Italia, pp 535–542

Malainey ME (2011) A consumer's guide to archaeological science: analytical techniques, manuals in archaeological method, theory and technique. Springer Science Business Media, New York

McKendry EM (2015) Interpreting Bronze Age exchange in Sicily through trace element characterization of ceramics utilizing portable X-ray fluorescence (pXRF). Thesis. University of South Florida

Mommsen H (2004) Short note: provenancing of pottery: the need for an integrated approach? Archaeometry 46(2):267–271

Neff H (2002) Quantitative techniques for analyzing ceramic compositional data. In: Glowacki DM, Neff H (eds) Ceramic production and circulation in greater southwest: source determination by INAA and complementary mineralogical investigations. Cotsen Institute of Archaeology, Los Angeles, pp 15–36

Newlander K, Goodale N, Jones TG, Bailey DG (2015) Empirical study of the effect of count time on the precision and accuracy of pXRF data. J Archaeol Sci Rep 3:534–548

Quinn P (2013) Ceramic petrography: the interpretation of archaeological pottery & related artefacts in thin section. Archaeopress, Oxford

Quinn P, Day PM (2007) Calcareous microfossils in Bronze Age Aegean ceramics: illuminating technology and provenance. Archaeometry 49(4):775–793

Raneri S, Barone G, Mazzoleni P, Tanasi D, Costa E (2015a) Mobility of men versus mobility of goods: archaeometric characterization of Middle Bronze Age pottery in Malta and Sicily (15th–13th century BC). Periodico di Mineralogia 84(1):23–44

Raneri S, Barone G, Crupi V, Longo F, Majolino D, Mazzoleni P, Tanasi D, Teixeira J, Venuti V (2015b) Technological analysis of Sicilian prehistoric pottery production through small angle neutron scattering technique. Periodico di Mineralogia 84(1):1–22

Rodrıguez C, Coronel-Prats RB, Barone G, Cultrone G, Mazzoleni P, Tanasi D (2015) Petrographic and chemical characterization of Bronze Age pottery from the settlement of Mount San Paolillo (Catania, Italy). Rend Fis Acc Lincei 26:485–497

Russell A (2017) Sicily without Mycenae: a cross-cultural consumption analysis of connectivity in the Bronze Age Central Mediterranean. J Mediterr Archaeol 30(1):59–83

Santacreu DA (2014) Materiality, techniques, and society in pottery production. De Gruyter Open, Berlin

Stovel EM, Cremonte B, Echenique E (2016) Petrography and pXRF at San Pedro de Atacama, Northern Chile: exploring ancient ceramic production. In: Ownby M, Masucci M (eds) Integrative approaches in ceramic petrography. University of Utah Press, pp 53–72

Tanasi D (2008) La Sicilia e l'arcipelago maltese nell'età del Bronzo Medio. Officina Studi Medievali, Palermo

Tanasi D (2010a) Gli scavi di Monte S. Paolillo e le presenze di tipo egeo nel territorio di Catania. In: La Rosa V, Branciforti MG (eds) Tra lava e mare. Contributi all'archaiologhia di Catania, Atti del Convegno, Catania, 22–23 novembre 2007, Catania: Le nove Muse, pp 81–94

Tanasi D (2010b) Bridging the gap. New data on the relationship between Sicily, the Maltese archipelago and the Aegean in the Middle Bronze Age. Mare Internum. Archeologia e culture del Mediterraneo 2:103–111

Tanasi D (2015) La storia di due colline: l'area della città di Catania nell'età del Bronzo Medio. In: Nicoletti F (ed) Catania Antica. Nuove prospettive di ricerca. Assessorato dei Beni Culturali e dell'Identità Siciliana, Palermo, pp 143–162

Tanasi D, Barone G, Mazzoleni P (2013) A case study for an archaeometric characterization of Sicilian Middle Bronze Age pottery (15th–13th C. BC). Swiatowit XI(LII):47–66

Tanasi D, Tykot RH, Pirone F, McKendry E (2017) Provenance study of prehistoric ceramics from Sicily: a comparative study between pXRF and XRF. Open Archaeol 3:222–234

Tusa S (2000) Ethnic dynamics during pre- and proto-history of Sicily. J Cult Herit 1:17–28

Tykot RH (2016) Using nondestructive portable X-ray fluorescence spectrometers on stone, ceramics, metals, and other materials in museums: advantages and limitations. Appl Spectrosc 70(1):42–56

Veca C (2014a) Per una tipo-tecnologia dei pithoi della meta II Millennio nella Sicilia Orientale. IpoTESI di Preistoria 6:195–208

Veca C (2014b) RSP LXIV:203–225

Veca C (2015) Innovation and tradition in technology of large storage jars of the Sicilian Middle Bronze Age. In: Proceedings of the XV SOMA (Catania University, 3–4 March 2011), BAR IS, 2695 (I), Archaeopress, pp 239–248

Whitbread IK (1986) The characterization of argillaceous inclusions in ceramic thin sections. Archaeometry 28:79–88

Whitbread IK (1989) A proposal for the systematic description of thin section towards the study of ancient ceramic technology. In: Maniatis Y (ed) 25th Hellenic Symposium on Archaeometry, Athens, 1986, pp 127–138